atmosphere

Article

Application of Portable CH_4 Detector Based on TDLAS Technology in Natural Gas Purification Plant

Yi Liu [1], Qianqian Shang [2], Lang Chen [2], Erxiao Wang [1], Xinyu Huang [1], Xiaobing Pang [2,*], Youhao Lu [2], Lei Zhou [2], Jue Zhou [2], Zhiwen Wang [2] and Yan Lyu [2]

1 Safety, Environment and Technology Supervision Research Institute of PetroChina Southwest Oil and Gas Field Company, Chengdu 610041, China; yiliu319@petrochina.com.cn (Y.L.); wangerxiao@petrochina.com.cn (E.W.); hxinyu0926@petrochina.com.cn (X.H.)

2 College of Environment, Zhejiang University of Technology, Hangzhou 310014, China; 2112127070@zjut.edu.cn (Q.S.); 2111927010@zjut.edu.cn (L.C.); 2112127082@zjut.edu.cn (Y.L.); 2112127157@zjut.edu.cn (L.Z.); 2112127205@zjut.edu.cn (J.Z.); 221122270108@zjut.edu.cn (Z.W.); yanlyu@zjut.edu.cn (Y.L.)

* Correspondence: pangxb@zjut.edu.cn

Abstract: Methane (CH_4) is the main pollutant in oil and gas production. The detection and accounting of CH_4 is an important issue in the process of greenhouse gas control and emission reduction in oil and gas industry. In this study, a portable CH_4 detector based on tunable diode laser absorption spectroscopy (TDLAS) technology was deployed. The three-dimensional distribution of CH_4 in a natural gas purification plant in Sichuan was obtained through vertical unmanned aerial vehicle (UAV) flight observations and ground mobile observations. According to the mass balance method, the emission of CH_4 on 30 m above ground level (AGL) and 60 m AGL in this site was about 0.012 kg/s (±42% at 1σ) and 0.034 kg/s (±47% at 1σ), respectively, in one day. The vertical distribution showed that the CH_4 concentration reached the maximum (2.75 ± 0.19 ppm) with height of 0 to 100 m AGL. The CH_4 concentration from 100 to 300 m AGL showed a downward trend with height. Atmospheric instability at high altitude and high wind speed promoted the diffusion of CH_4. The CH_4 concentrations of horizontal distribution on 30 m AGL and 60 m AGL were 2.48 ± 0.11 ppm and 2.76 ± 0.34 ppm. In the observation of mobile campaigns, the connecting equipment of natural gas treatment facilities was prone to leakage, such as in valves and flanges. CH_4 leakage was also detected at the torch mouth, especially when there was an open flame at the torch mouth. During the mobile movement investigation, the downwind measurement (OTM-33A) was applied to determine the overall CH_4 emission rate shortly after patrolling the site. This work plays a vital role in optimizing the operation and maintenance of natural gas production stations pipe network, ensuring human safety and minimizing greenhouse gas emissions.

Keywords: methane; natural gas purification plant; tunable diode laser absorption spectroscopy; unmanned aerial vehicle flight observation; spatial distribution

Citation: Liu, Y.; Shang, Q.; Chen, L.; Wang, E.; Huang, X.; Pang, X.; Lu, Y.; Zhou, L.; Zhou, J.; Wang, Z.; et al. Application of Portable CH_4 Detector Based on TDLAS Technology in Natural Gas Purification Plant. *Atmosphere* **2023**, *14*, 1709. https://doi.org/10.3390/atmos14121709

Received: 7 October 2023
Revised: 12 November 2023
Accepted: 17 November 2023
Published: 21 November 2023

1. Introduction

Methane (CH_4) is a potential greenhouse gas. Since the pre-industrial era, the emission of CH_4 from human activities has caused a radiation force of 0.97 W/m^2, compared with the emission of carbon dioxide (CO_2) of 1.7 W/m^2 [1]. The global emissions of CH_4 in the world is about 5.7×10^8 t, of which 60% comes from anthropogenic emissions [2]. According to isotopic signature measurements of ice core and accumulated snow samples to assess pre-industrial CH_4 levels, the extent of the increase in anthropogenic fossil fuel CH_4 emissions may be underestimated by 25–40% [3,4]. Oil and natural gas systems (ONGs) are the leading CH_4 emission source in the field of energy supply, with emissions of 1677.3 $MtCO_2eq$ in 2010 [5].Therefore, it is of great significance to improve the performance of CH_4 detection technology to avoid destructive losses and atmospheric pollutants caused by CH_4 leakage in the petroleum and petrochemical industries. From the producer's point of view, natural gas leakage also means the loss of products and income.

The vehicle-mounted method has the advantages of having no need to enter the station, large detection coverage and accurate location of CH_4 leakage. MacKay et al. measured CH_4 emissions from 6650 locations in six major oil and gas producing areas in Canada by vehicle-mounted measurement [6]. Yacovitch et al. continuously measured and estimated the location of CH_4 emission at 224 locations in Banert through a mobile laboratory [7]. Thoma et al. used GMAP-REQ platform with a G1301-fc cavity ring-down spectrometer to measure the emissions from well sites in Texas, Colorado and Wyoming. The results showed that the median CH_4 emission rates were 0.43 g/s, 0.21 g/s and 0.79 g/s, respectively [8]. All the above studies are based on ground measurement to investigate CH_4 emissions. However, these mobile laboratories and ground investigation technologies are more time-consuming or may miss high leakage sources.

In recent years, airborne-based platforms, such as manned light aircraft, have effectively capture lofted plumes [9,10]. Karion et al. used airborne measurement technology to measure the regional CH_4 emissions from oil and gas operations in Banert shale, Texas, USA [11]. Allen et al. used the component-level and vehicle-mounted tracer method to detect the oil and gas production stations in the United States, and the average daily natural gas production of the covered production stations ranged from 5.6×10^2 to 1.33×10^6 m^3 [12]. Yuan et al. the airborne measurement method to measure CH_4 emission from two shale gas fields in the United States [13]. However, for the sake of public safety and property losses, it is not allowed to fly at ultra-low altitude or near the source. CH_4 emissions from shale gas producing areas in the United States are measured by the Picarro measurement system on a plane This expensive instrument is not easily accessible to most scientists, and it is too large to be carried for outdoor experiments [14]. Therefore, it is urgent to develop a CH_4 detector with high precision, low cost and real-time monitoring.

Laser-based techniques, also known as laser absorption spectroscopy (LAS), achieve selectivity for a target gas, typically CH_4 [15]. The most common LAS technology is called tunable diode laser absorption spectroscopy (TDLAS) [16]. In 2002, TDLAS techniques and dual-frequency modulated spectroscopy were used to analyze atmospheric gases [17]. Titchener et al. reported a new type of remote sensor using single photon lidar and TDLAS, which was used to continuously monitor the unorganized emission of industrial CH_4 [18]. Zhang et al. applied an NIR-TDLAS spectrometer to locate and quantify the unorganized emission of oil and gas fields [19]. In this study, we deployed a portable CH_4 detector based on TDLAS technology. On April 2023, we observed the three-dimensional CH_4 distribution of a natural gas purification plant in Sichuan Province, China. Combined with UAV flight and mobile monitoring activities, the vertical and spatial distributions of CH_4 in the natural gas purification plant was comprehensively observed. The mass balance method and Other Test Method 33A (OTM 33A) were used to calculate and evaluate CH_4 emission flux. The purpose of this study is to develop a new measuring system to investigate CH_4 emissions from natural gas purification plants and provide reliable basic data and a more scientific basis for policies to alleviate global warming.

2. Materials and Methods

2.1. Sampling Site

The sampling site was located in an oil and gas mine in Sichuan, China (Figure 1). The plant is mainly responsible for treating and purifying the primary natural gas extracted from oil and gas mines, with an average daily output of 4.45×10^6 m^3. The natural gas purification plant is divided into seven main links: pre-treatment, membrane separation, adsorption, desulfurization and decarbonization, dehydration and the production of liquefied natural gas.

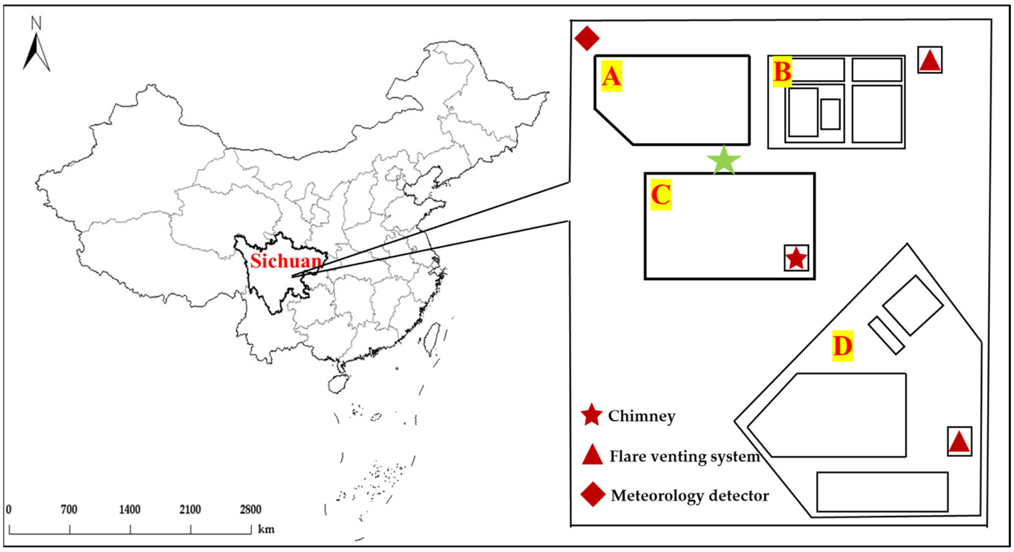

Figure 1. Location of observation point of natural gas purification plant in Sichuan Province, China. Areas A and C are the main production equipment areas, which refer to the natural gas purification equipment areas, with processing capacity of 1.3×10^6 m^3/d and 3.0×10^6 m^3/d, respectively. Areas B and D are auxiliary production equipment areas, such as sulfur molding and warehouse, circulating water device, sewage treatment device, air compressor and so on. The bold black line surrounding area A and area C represents the path of horizontal measurement at high altitude and mobile observation of CH_4.

2.2. Apparatus

According to Figure 2, we deployed a portable CH_4 detector (Tengyork, Shaoxing, China, http://www.tengyork.com/product/id/8vuz3.html, accessed on 20 November 2023) based on TDLAS technology, which is a method of scanning the laser wavelength around the specific absorption line. In the working state, the laser signal is absorbed by methane gas, and the concentration value of methane gas can be accurately deduced by the change of laser absorption spectrum. All detector signals were collected and converted by a data-acquisition device through a microcomputer. The detailed parameters of the portable CH_4 detector are shown in Table 1.

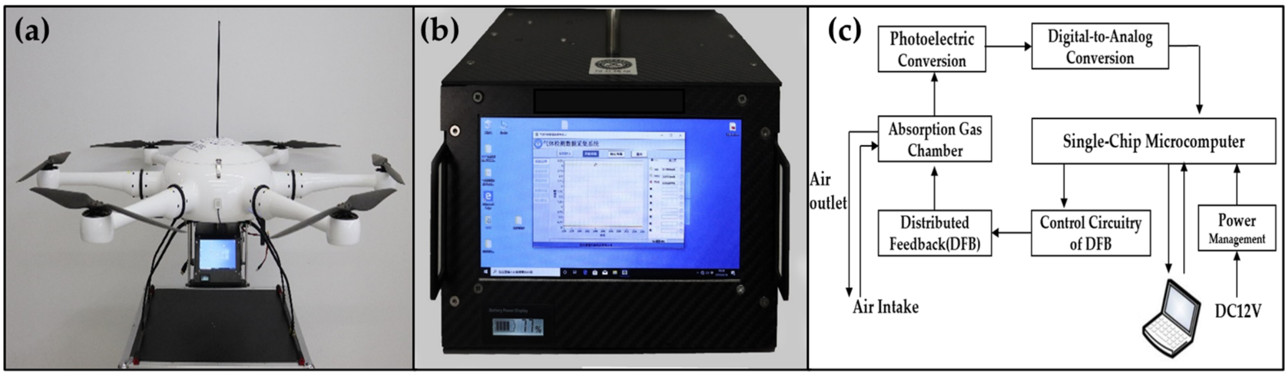

Figure 2. (**a**) The self-developed CH_4 detector is installed on the UAV for aerial monitoring of a natural gas purification plant in Sichuan Province, China. (**b**) The self-developed CH_4 detector (**c**) The internal working principle of the CH_4 detector.

Table 1. The performance parameters of CH_4 detector.

Category	Detailed Parameters
Size	13 (length) × 20 (width) × 29 cm (height)
Overall weight	2 kg
Operating voltage	12 V
Sampling flow	0.4~0.6 L/min
Range of detection	0~100 ppm
Measurement error	±1%
Precision	0.01 ppm
Time of response	≤1 s
Endurance	10 h
Pump	19 (width) × 53.2 mm (length), 23.1 g
Sheathing material	Carbon fiber
Cost of investment	$14,000

A six-rotor UAV was selected to carry the CH_4 detector in this field campaign (Figure 2), and the air inlet of the CH_4 detector was located 0.6 m above the UAV to alleviate the air turbulence effect caused by the downwash of the UAV rotor [20]. The detailed parameters of the UAV are shown in Table 2. The meteorological parameters of the natural gas purification plant were observed by using a three-dimensional ultrasonic wind speed and direction meter (M307200) and a portable meteorological detector (Figure 1).

Table 2. The performance parameters of UAV.

Category	Detailed Parameters
Size	60 (height) × 230 cm (width)
Material	Carbon fiber
Endurance	0.5 h
Maximum load weight	6 kg
Maximum flying altitude	500 m
Farthest plane flight distance	1000 m
Flight control system	DJI-A3
Image and control system	DJI-lightbridge2
Cost of investment	$20,000

2.3. Experimental Process

2.3.1. Vertical Measurement of CH_4

To study the vertical distribution of CH_4 at different times, we carried out vertical flight experiments at 9:00, 11:00, 13:00, 15:00, 17:00 and 19:00 local time (LT), respectively, in April 2023. According to Figure 3, in each vertical flight, the UAV raised vertically to 300 m AGL and hovered for 1 min (min), then began to descend, hovering for 1 min at the heights of 200, 100 and 50 m AGL, respectively, and returning to the ground. According to Figure 1, the position of vertical flight is between area A and area C, which is indicated by a green five-pointed star.

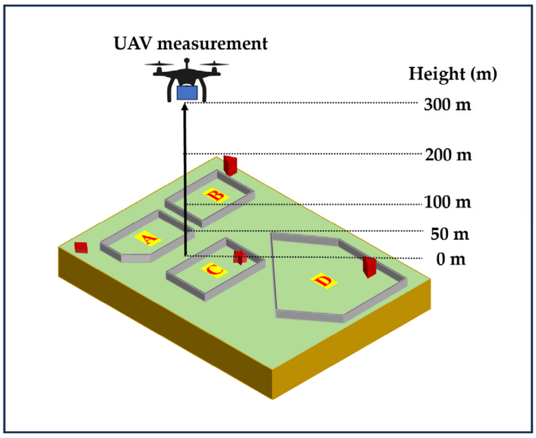

Figure 3. Schematic diagram of vertical measurement of CH_4 by UAV equipped with CH_4 detector.

2.3.2. Horizontal Measurement of CH_4

The experimenter controlled the UAV equipped with CH_4 detector to conduct detection around area A and area C at the speed of 1 m/s, respectively. The heights were determined to be 30 m and 60 m AGL, which can cover the potential leakage area to the greatest extent. When setting the detected height, the following factors should be considered: detected target, safe distance (stay away from natural gas equipment and pipelines) and environmental factors (such as meteorology, wind speed, airflow, etc.). The meteorological factors during the experiment are shown in Figure 4. ABLH is the abbreviation for atmospheric boundary layer height. According to the downward shortwave radiation flux (DSRF) and the wind speed, the PS classification was determined [21].

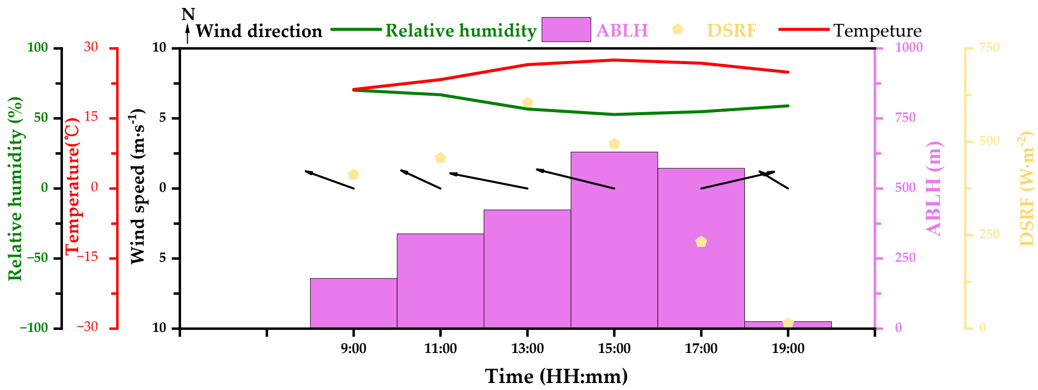

Figure 4. The experimental dates correspond to meteorological conditions and atmospheric stability (PS classification).

2.3.3. Measurement of CH_4 from the Torches and Chimneys

The pilot maneuvered the drone into the plume (about 50 m AGL) and measured CH_4 online by flying. The flight time lasted about 10 min. The UAV hovered over the vent, and the vertical distances between the UAV and the vent of the torch and chimney were controlled at 6 m and 2 m, respectively.

2.3.4. Mobile Observation of CH_4

The CH_4 mobile monitoring campaigns were periodically conducted on 13 April 2023, at six periods of one day (9:00, 11:00, 13:00, 15:00, 17:00 and 19:00 LT). The speed of mobile observation was controlled at 10 km/h to ensure that CH_4 in the atmosphere reacted with the device. The sample height was designed at 1 m AGL. The whole experimental route was approximately 2 km, including the daily inspection route in the factory, pipeline valves and flange joints of the natural gas purification devices.

2.3.5. Flux Quantification of CH_4

The most common flux estimation method for UAV is the mass balance method [19], which derives the net flux by integrating the measured concentration (above background level) across a vertical sampling plane downwind of the emitting source. The total flux (in moles/s) of CH_4 was calculated as:

$$\mathrm{Flux} = \int_0^Z \int_A^B (S_{ij} - S_0) n_{ij} U_{\perp ij} dxdz \tag{1}$$

where S_{ij} is the mole fraction (moles/mole) of species S for each coordinate on the vertical plane AB (oriented perpendicular to the prevailing mean wind vector), and S_0 is the measured (or assumed) background. The n_{ij} term is the mole density of air (moles·m^{-3}), which is determined using an ideal gas assumption. The $U_{\perp ij}$ term is the wind speed (m·s^{-1}) perpendicular to a downwind vertical horizontal plane AB. Fluxes are then integrated over the vertical and horizontal (AB) extent of the plane (or plume) to calculate flux through this plane.

The measurement of CH_4 emission from ground movement was usually carried out in the downwind of the station to obtain the concentration for the whole natural gas station or area. The Environmental Protection Agency (EPA) proposed another test method, 33A (OTM-33A) [22], a programmed version of the downwind measurement method, making it easy to apply for researchers or operational personnel [23]. The emission rate was calculated as:

$$Q = 2\pi \times \overline{U} \times \sigma_Y \times \sigma_Z \times C_{peak} \tag{2}$$

where Q is the CH_4 emission rate (kg/h), $\overline{U}$ is the average wind speed (m/s), and σ_Y and σ_Z are the horizontal and vertical dispersion coefficients, respectively, determined based on the average local atmospheric stability class and the measured downwind distance. The CH_4 background concentration was determined as the lowest 5% of all concentration data and subtracted. A Gaussian fit of the concentration enhancement versus the wind direction was performed with the vertex of the fit as C_{peak}. The above procedures were performed using the MATLAB program code provided by the OTM-33A manual [24].

2.4. Data Quality Assurance

Before the measurement, the CH_4 detector was calibrated in the laboratory to improve its accuracy. The known concentrations of the CH_4 standard gases were passed into the CH_4 detector until stable gas concentration data were obtained, and the stabilization time was 3 min. To verify the reliability of the CH_4 detector, the standard gases produced by the reference device at six concentrations (0, 2, 4, 6, 8 and 10 ppm) were measured by a sensor. Then, standard curves were made to determine the calibration effect. After calibration, the CH_4 detector shows good agreement with a linear regression correlation coefficient (R^2) up to 0.99.

3. Results and Discussion

3.1. High-Altitude Emission of CH_4

The vertical distribution of CH_4 concentrations in the natural gas purification plant is shown in Figure 5. The CH_4 concentration gradually increased to the maximum (2.75 ± 0.19 ppm) from 0 to 100 m AGL and then began to decrease. The concentration of CH_4 at 60 m AGL (2.76 ± 0.34 ppm) was higher than 30 m AGL (2.48 ± 0.11 ppm). The CH_4 concentration at 300 m AGL was 2.52 ± 0.11 ppm, which was lower than the ground. The density of CH_4 is lower than that of air, and it generally rises near the ground. Leakage of equipment near the ground may also be one of the reasons. Flange connection is mostly used between natural gas pipelines or between pipelines and equipment, which is also the most vulnerable part for natural gas leakage. During the mobile observation at the site, CH_4 leakage was found in many flanges, joints and grease holes (Figure 6).

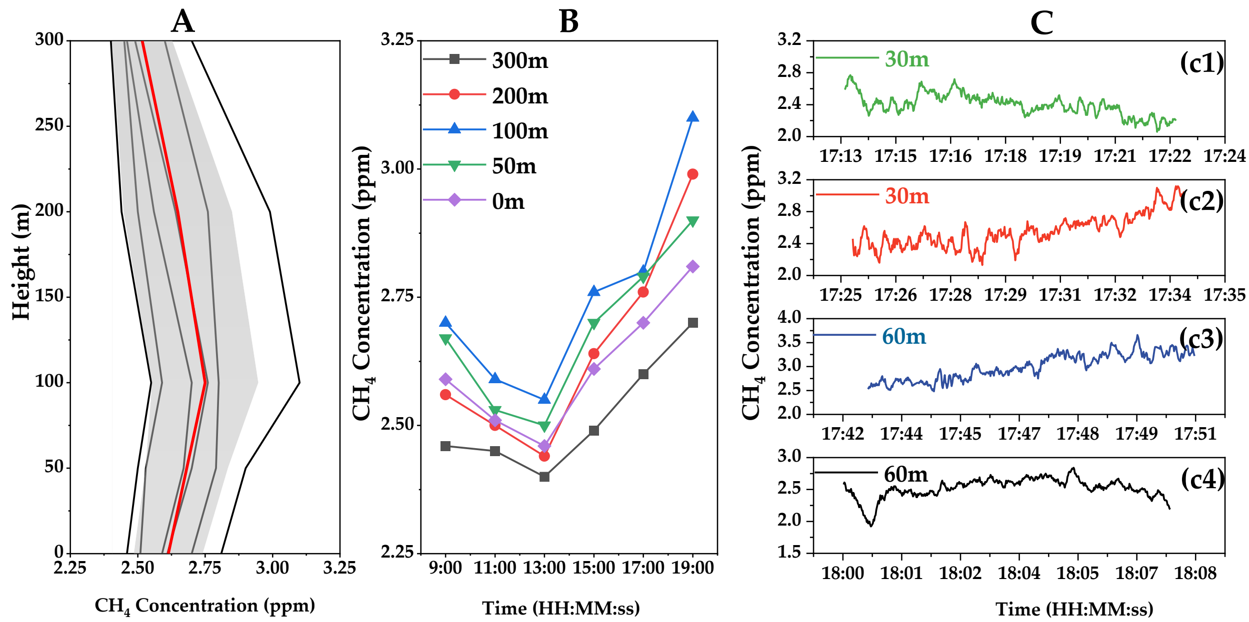

Figure 5. (**A**) The vertical profiles of CH_4 concentrations at different times. The black line represents the concentration changes of a single vertical observation, the red line is the mean value and the shaded areas are the standard deviations. (**B**) Diurnal variation of CH_4 concentration at different heights. (**C**) The UAV equipped with CH_4 detector hovered over the natural gas purification plant on 13 April 2023. (**c1**,**c2**) represent the first and second horizontal measurement of CH_4 at 30 m AGL respectively. (**c3**,**c4**) represent the first and second horizontal measurement of CH_4 at 60 m AGL respectively.

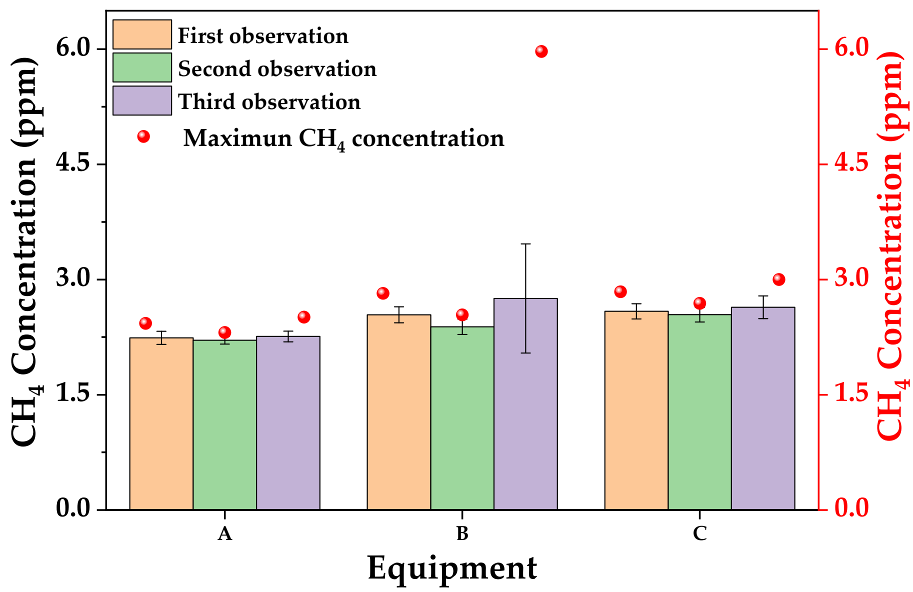

Figure 6. The average concentration of CH_4 in chimneys and torches. A represent chimney, and B and C represent torch. Each test point was measured 3 times.

The daily variation of CH_4 at different heights is shown in Figure 5B. At 11:00 LT, the CH_4 concentration began to decrease, and the relative increase of atmospheric boundary layer height and wind speed after sunrise acted as the diffusion agent for atmospheric CH_4 molar fraction [25]. The CH_4 concentration decreased to the minimum at 13:00 LT, which was similar to the daily cycle observed in Shanghai, China [26]. As shown in Figure 4, the DSRF reached the maximum value of 604 W/m^{-2} at 13:00 LT. Active photochemical reactions can reduce the concentration of CH_4. The dominant loss of CH_4 was through oxidation in the atmosphere via the hydroxyl radical (OH). Active photochemical reactions can consume a certain concentration of oxygen. CH_4 is a reductive gas, and it is easily oxidized in the atmosphere [27]. The CH_4 concentration began to rise at 17:00 LT, but its growth rate was lower than 19:00 LT. At 19:00 LT, the atmosphere was relatively stable (PS = D), which hindered the vertical diffusion of CH_4 and increased it [28]. In addition, the low wind speed and ABLH were also reasons for the high CH_4 concentration at night [29,30].

The CH_4 concentration of chimneys and flares in the natural gas purification plant is shown in Figure 5. The CH_4 concentrations at the discharge ports of the chimney (A) and torches (B and C) were 2.24 $\pm$ 0.03, 2.60 $\pm$ 0.35 and 2.59 $\pm$ 0.03 ppm respectively. The CH_4 concentration of the two torches was higher than that of the chimney. In the third observation of torch B, it was found that the CH_4 concentration increased obviously, reaching a maximum of 5.97 ppm, indicating that there was a leak. Compared with torch B, the change of CH_4 concentration in torch C was relatively stable.

3.2. Spatial Distribution of CH_4

The measurement of CH_4 from ground movement was usually carried out in the downwind of the station to obtain the CH_4 concentration for the whole natural gas station or area.

The observation results of CH_4 movement in the natural gas purification plant are shown in Figure 7. The average CH_4 concentrations at 9:00 LT and 11:00 LT were 2.39 $\pm$ 0.38 ppm and 2.17 $\pm$ 0.05 ppm, respectively, both of which were lower than those at 19:00 LT (2.64 $\pm$ 0.27 ppm). At 13:00 LT, the CH_4 concentration exceeded 3.0 ppm in 33 places outside area A and inside area C. Interestingly, the CH_4 concentration at 13:00 LT was the lowest (2.47 $\pm$ 0.06 ppm) in a single day according to the Figure 5, which showed that the mobile observation supplemented the high-altitude monitoring data to some extent. According to Figure 8, the CH_4 concentration in the station increased obviously at 15:00 LT and 17:00 LT, with 47.2% and 43.5% of CH_4 exceeding 3 ppm, respectively. The CH_4 concentration of gas pipeline valves were relatively high in the natural gas purification unit area (Area A). The valve is affected by the temperature, pressure, erosion and vibration corrosion of natural gas, and the defects in the production and manufacture of the valve will inevitably lead to CH_4 leakage in the process of use [31]. In the natural gas purification unit area (area C), the maximum concentration of CH_4 was 394.48 ppm, and the leakage point was located at the product gas delivery flange. Flange connection is the main form of natural gas pipeline and equipment connection, and its leakage is also one of the most important forms of natural gas station leakage. The sealing of the flange mainly depends on the pre-tightening force generated by the bolt connected with it, and the gasket can achieve enough working sealing specific pressure to prevent natural gas leakage [32]. For the natural gas pipeline, the transmission medium has the characteristics of corrosion, high pressure and vibration during transportation, which will lead to the failure of the flange seal o for the natural gas pipeline and leakage [32].

The mobile movement observation of CH_4 can achieve a large coverage in the detection range. However, due to the randomness of CH_4 emission, short-term "snapshot" on-site mobile detection may not capture this CH_4 emission signal. It is necessary to take longer-term (2 weeks or more) CH_4 emission detection measures in the future [33].

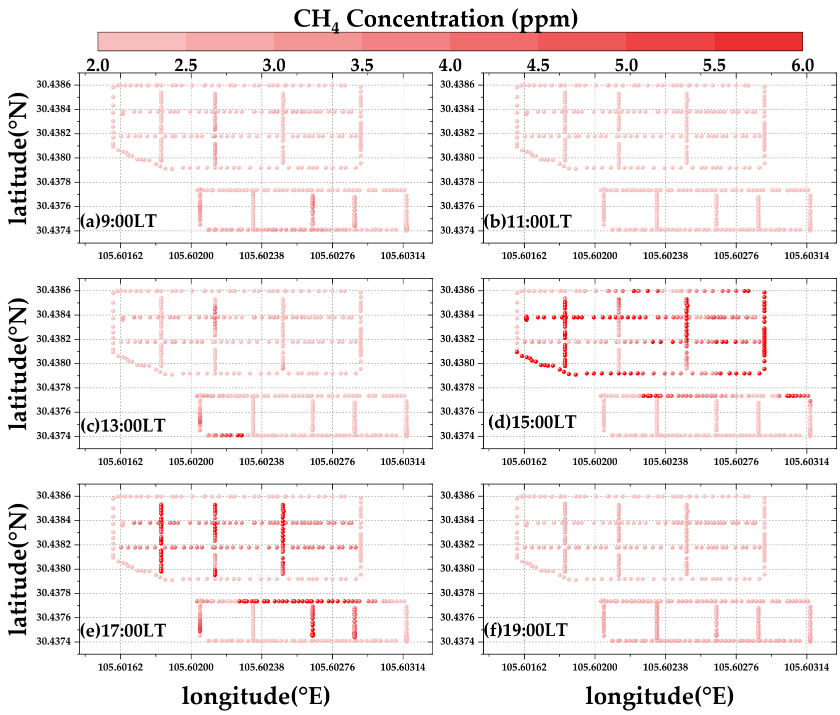

Figure 7. CH_4 concentration trajectories detected by the portable CH_4 detector during the mobile monitoring campaign in the natural gas purification plant.

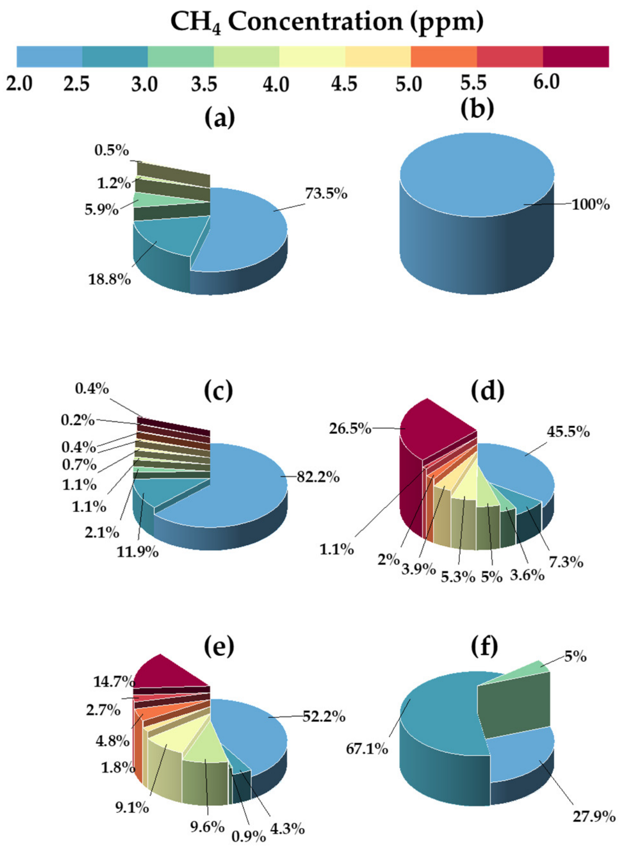

Figure 8. Proportion of CH_4 concentration range in mobile observation. The time from (**a**–**f**) corresponds to Figure 7.

3.3. Flux Quantification of CH_4

The spatially-interpolated CH_4 enhancement projected onto the flux planes is shown in Figure 9. Having obtained the spatially interpolated flux planes downwind (with the mean background subtracted to represent net downwind enhancement) in Figure 9, Equation (1) was used to calculate CH_4 flux by integrating across the horizontal and vertical extents of the 2D sampling plane perpendicular to the prevailing wind. In the observation of mobile measurement, the background concentration of CH_4 was determined to be 2.03 ppm (the lowest 5% of all concentration data). The concentration of CH_4 at 60 m AGL (2.76 ± 0.34 ppm) in the natural gas purification plant was higher than 30 m AGL (2.48 ± 0.11 ppm). In the Lagrange mass balance method, the amount of air entering and leaving an air volume is measured with the difference of measured values, thus giving the net surface flux in the volume. According to Table 3, for the flight on 30 m AGL, the flux was derived to be 0.012 kg/s (±42% at 1σ) with an uncertainty dominating in both the background variability (accounting for 63% of the total flux uncertainty) and the wind measurement variability (accounting for 19% of the total flux uncertainty). For the flight on 60 m AGL, the flux was derived to be 0.034 kg/s (±47% at 1σ) with an uncertainty dominating in the background variability (accounting for 82% of the total flux uncertainty).

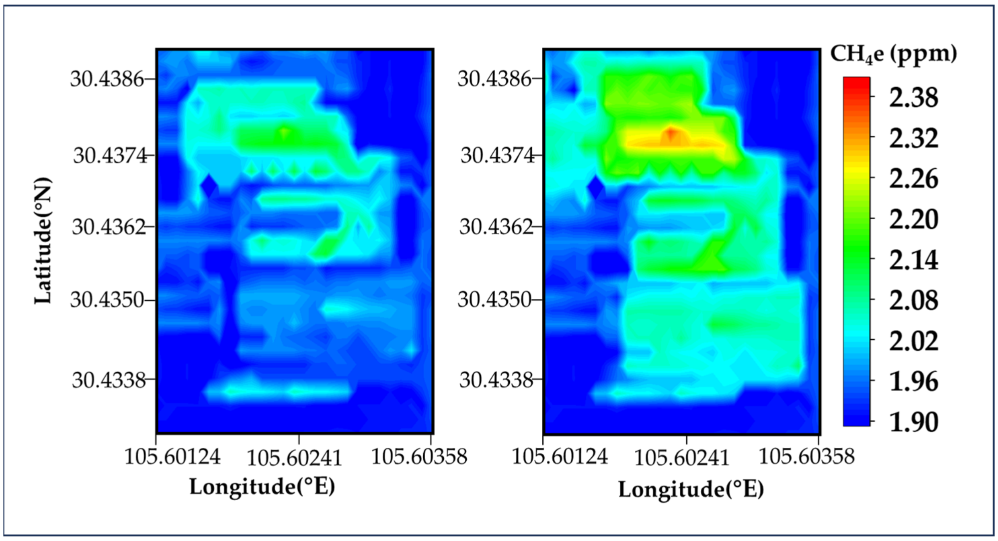

Figure 9. Background CH_4 enhancement (CH_4e) spatially interpolated on 30 m AGL (left panel) and 60 m AGL (right panel) of UAV flight (in units of ppm as per color scale).

Table 3. Mean CH_4 flux and one standard deviation uncertainties.

Units in kg/s	Height of Flight	
	30 m AGL	60 m AGL
Mean flux	0.012	0.034
total uncertainty	0.00504	0.01598
Wind uncertainty	0.0009576	0.0003995
Background uncertainty	0.0031752	0.0131036
Measurement uncertainty	0.0001008	0.0003196
Downwind uncertainty	0.0008064	0.00204544

3.4. Treatment and Preventive Measures for Equipment Leakage

In view of the natural gas leakage in the flange, the bolts can be tightened by depressurizing and venting. If it is necessary to stop gas transmission, the valves on both sides of the leaking part must be closed, the old gasket should be replaced after venting, and then the bolts should be tightened again. In the case that gas transmission can not be stopped, flange plugging treatment technology is needed to deal with it. According to the actual leakage situation, in order to avoid more leakage, it is best to use a wound metal flange gasket or metal ring gasket. In view of the valve leakage, it can be dealt with by fastening bolts. There is too much purge gas in the emergency torch, so it is necessary to install a more reliable automatic ignition system and adjust the purge gas to the minimum required level. Preventive measures can be taken against the leakage of natural gas pipelines. For example, the cleaning of natural gas pipeline in the future can avoid the existence of iron sulfide powder in the pipeline. When the peak gas consumption comes in winter, it is necessary to prepare for standby gas to protect the gas pipeline from flying dust due to the excessive gas flow rate, resulting in excessive wear and tear of the pipeline.

4. Conclusions

In this study, a lightweight (<3 kg), low-cost ($14,000), and portable CH_4 detector based on TDLAS technology was developed. We made many aerial and ground investigations on a natural gas station in Sichuan, China by using a self-developed CH_4 detector. The results show that, in vertical detection, the CH_4 concentration increased with height at 0 to 100 m AGL and decreased at 100 to 300 m AGL. In the horizontal measurement, the CH_4 emission flux at 30 m AGL and 60 m AGL were approximately 0.012 kg/s (±42% at 1σ) and 0.034 kg/s (±47% at 1σ), respectively, in a day. However, this calculation method is not necessarily accurate. Uncertainty contributing to the flux was dominated by ambient variability in the background (inflow) concentration (>60%) and wind speed (>20%), with instrumental error contributing about 1–2%. CH_4 leakage was detected at the torch mouth, especially when there was an open flame at the torch mouth. During the mobile observation, we found leakage at the flange and valve some of the time.

The UAV equipped with CH_4 detector can go deep into some areas that are difficult for personnel to reach in order to carry out monitoring activities, thus improving the working efficiency. With the aid of mobile observation, CH_4 emission from natural gas stations can be better detected. Another advantage is that the time resolution of the instrument is 1 s, which captures the fine and dynamic spatial changes of CH_4. This study is helpful for oil field production enterprises in carrying out effective and reliable CH_4 emission reduction.

In addition, this study was conducted at a certain time in the day, which may affect the applicability of this measurement method in other places. Ground-based meteorological sensors may not provide the necessary spatial and vertical resolution, and winds should ideally be measured onboard the UAV in the future. Besides, it is necessary to expand the temporal and spatial coverage of this study to answer the complete distribution of CH_4 and the emission factors of components in normal and abnormal activities.

Author Contributions: Y.L. (Yi Liu): Conceptualization, Data curation, Writing—original draft preparation; Q.S.: Writing-review and editing, Supervision; E.W.: Data curation; X.H.: Data curation; L.C.: Conceptualization, Writing—review and editing, Funding acquisition, Supervision, Project administration; E.W.: Data curation, Software editing; X.H.: Data curation, Software editing; X.P.: Writing—review and editing, Data curation, Software editing, project investigation, project administration; Y.L. (Youhao Lu): project investigation; L.Z.: project investigation; J.Z.: Software editing; Z.W.: Software editing; Y.L. (Yan Lyu): Software editing. All authors have read and agreed to the published version of the manuscript.

Funding: This work was supported by the National Natural Science Foundation of China (42327806), Chongqing Technological Innovation and Application Development Special Key Project (CSTB2022TIAD-CUX0010), Zhejiang Province Lingyan Research and Development Project (2022C03073), and Shaoxing Science and Technology Plan Project (2022B41006).

Institutional Review Board Statement: Not applicable.

Informed Consent Statement: Not applicable.

Data Availability Statement: The data presented in this study are available on request from the corresponding author. The data are not publicly available due to the fact that the study continues and the data is still being worked on.

Conflicts of Interest: Authors Yi Liu, Erxiao Wang, Xinyu Huang are employed by Safety, Environment and Technology Supervision Research Institute of PetroChina Southwest Oil and Gas Field Company. The remaining authors declare that the research was conducted in the absence of any commercial or financial relationships that could be construed as a potential conflict of interest.

References

1. Alvarez, R.A.; Zavala-Araiza, D.; Lyon, D.R.; Allen, D.T.; Barkley, Z.R.; Brandt, A.R.; Davis, K.J.; Herndon, S.C.; Jacob, D.J.; Karion, A.; et al. Assessment of methane emissions from the US oil and gas supply chain. *Science* **2018**, *361*, 186–188.
2. Erland, B.M.; Thorpe, A.K.; Gamon, J.A. Recent Advances Toward Transparent Methane Emissions Monitoring: A Review. *Environ. Sci. Technol.* **2022**, *56*, 16567–16581. [CrossRef]
3. Petrenko, V.V.; Smith, A.M.; Schaefer, H.; Riedel, K.; Brook, E.; Baggenstos, D.; Harth, C.; Hua, Q.; Buizert, C.; Schilt, A.; et al. Minimal geological methane emissions during the Younger Dryas-Preboreal abrupt warming event. *Nature* **2017**, *548*, 443–446. [CrossRef]
4. Hmiel, B.; Petrenko, V.V.; Dyonisius, M.N.; Buizert, C.; Smith, A.M.; Place, P.F.; Harth, C.; Beaudette, R.; Hua, Q.; Yang, B.; et al. Preindustrial, (CH_4)-C-14 indicates greater anthropogenic fossil CH_4 emissions. *Nature* **2020**, *578*, 409. [CrossRef]
5. Chen, G.; Yang, S.; Lv, C.; Zhong, J.; Wang, Z.; Zhang, Z.; Fang, X.; Li, S.; Yang, W.; Xue, L. An improved method for estimating GHG emissions from onshore oil and gas exploration and development in China. *Sci. Total Environ.* **2017**, *574*, 707–715. [CrossRef]
6. Mackay, K.; Lavoie, M.; Bourlon, E.; Atherton, E.; O'connell, E.; Baillie, J.; Fougere, C.; Risk, D. Methane emissions from upstream oil and gas production in Canada are underestimated. *Sci. Rep.* **2021**, *11*, 8041. [CrossRef]
7. Yacovitch, T.I.; Herndon, S.C.; Petron, G.; Kofler, J.; Lyon, D.; Zahniser, M.S.; Kolb, C.E. Mobile Laboratory Observations of Methane Emissions in the Barnett Shale Region. *Environ. Sci. Technol.* **2015**, *49*, 7889–7895. [CrossRef]
8. Thoma, E.D.; Squier, B.C.; Olson, D.; Eisele, A.P.; Dewees, J.M.; Segall, R.R.; Amin, M.S.; Modrak, M.T. Assessment of Methane and VOC Emissions from Select Upstream Oil and Gas Production Operations Using Remote Measurements, Interim Report on Recent Survey Studies. In Proceedings of the 105th Annual Conference on Air Waste Management Assocociation, Durham, NC, USA, 24–26 April 2012.
9. Xueref-Remy, I.; Zazzeri, G.; Bréon, F.M.; Vogel, F.; Ciais, P.; Lowry, D.; Nisbet, E.G. Anthropogenic methane plume detection from point sources in the Paris megacity area and characterization of their $\delta^{13}C$ signature. *Atmos. Environ.* **2020**, *222*, 117055. [CrossRef]
10. Pangerl, J.; Müller, M.; Rück, T.; Weigl, S.; Bierl, R. Characterizing a sensitive compact mid-infrared photoacoustic sensor for methane, ethane and acetylene detection considering changing ambient parameters and bulk composition, (N_2, O_2 and H_2O). *Sens. Actuators B Chem.* **2022**, *352*, 130962. [CrossRef]
11. Karion, A.; Sweeney, C.; Kort, E.A.; Shepson, P.B.; Brewer, A.; Cambaliza, M.; Conley, S.A.; Davis, K.; Deng, A.; Hardesty, M.; et al. Aircraft-Based Estimate of Total Methane Emissions from the Barnett Shale Region. *Environ. Sci. Technol.* **2015**, *49*, 8124–8131. [CrossRef]
12. Allen, D.T.; Torres, V.M.; Thomas, J.; Sullivan, D.W.; Harrison, M.; Hendler, A.; Herndon, S.C.; Kolb, C.E.; Fraser, M.P.; Hill, A.D.; et al. Measurements of methane emissions at natural gas production sites in the United States. *Proc. Natl. Acad. Sci. USA* **2013**, *110*, 17768–17773. [CrossRef]
13. Yuan, B.; Kaser, L.; Karl, T.; Graus, M.; Peischl, J.; Campos, T.L.; Shertz, S.; Apel, E.C.; Hornbrook, R.S.; Hills, A.; et al. Airborne flux measurements of methane and volatile organic compounds over the Haynesville and Marcellus shale gas production regions. *J. Geophys. Res. Atmos.* **2015**, *120*, 6271–6289. [CrossRef]
14. Peischl, J.; Ryerson, T.B.; Aikin, K.C.; Gouw, J.A.; Gilman, J.B.; Holloway, J.S.; Lerner, B.M.; Nadkarni, R.; Neuman, J.A.; Nowak, J.B.; et al. Quantifying atmospheric methane emissions from the Haynesville, Fayetteville, and northeastern Marcellus shale gas production regions. *J. Geophys. Res. Atmos.* **2015**, *120*, 2119–2139. [CrossRef]
15. Wang, F.; Jia, S.; Wang, Y.; Tang, Z. Recent Developments in Modulation Spectroscopy for Methane Detection Based on Tunable Diode Laser. *Appl. Sci.* **2019**, *9*, 2816. [CrossRef]
16. Burgues, J.; Marco, S. Environmental chemical sensing using small drones: A review. *Sci. Total Environ.* **2020**, *748*, 141172. [CrossRef]
17. D'amato, F.; De Rosa, M. Tunable diode lasers and two-tone frequency modulation spectroscopy applied to atmospheric gas analysis. *Opt. Lasers Eng.* **2002**, *37*, 533–551. [CrossRef]
18. Titchener, J.; Millington-Smith, D.; Goldsack, C.; Harrison, G.; Dunning, A.; Ai, X.; Reed, M. Single photon Lidar gas imagers for practical and widespread continuous methane monitoring. *Appl. Energy* **2022**, *306*, 118086. [CrossRef]
19. Allen, G.; Hollingsworth, P.; Kabbabe, K.; Pitt, J.R.; Mead, M.I.; Illingworth, S.; Roberts, G.; Bourn, M.; Shallcross, D.E.; Percival, C.J. The development and trial of an unmanned aerial system for the measurement of methane flux from landfill and greenhouse gas emission hotspots. *Waste Manag.* **2019**, *87*, 883–892. [CrossRef]

20. Pang, X.; Chen, L.; Shi, K.; Wu, F.; Chen, J.; Fang, S.; Wang, J.; Xu, M. A lightweight low-cost and multipollutant sensor package for aerial observations of air pollutants in atmospheric boundary layer. *Sci. Total Environ.* **2021**, *764*, 142828. [CrossRef]
21. Nakajima, K.; Yamanaka, T.; Ooka, R.; Kikumoto, H.; Sugawara, H. Observational assessment of applicability of Pasquill stability class in urban areas for detection of neutrally stratified wind profiles. *J. Wind. Eng. Ind. Aerodyn.* **2020**, *206*, 104337. [CrossRef]
22. Robertson, A.M.; Edie, R.; Snare, D.; Soltis, J.; Field, R.A.; Burkhart, M.D.; Bell, C.S.; Zimmerle, D.; Murphy, S.M. Variation in Methane Emission Rates from Well Pads in Four Oil and Gas Basins with Contrasting Production Volumes and Compositions. *Environ. Sci. Technol.* **2017**, *51*, 8832–8840. [CrossRef]
23. Edie, R.; Robertson, A.M.; Field, R.A.; Soltis, J.; Snare, D.A.; Zimmerle, D.; Bell, C.S.; Vaughn, T.L.; Murphy, S.M. Constraining the accuracy of flux estimates using OTM 33A. *Atmos. Meas. Tech.* **2020**, *13*, 341–353. [CrossRef]
24. *MATLAB*, Version 8.5.0, (R2015a); The MathWorks Inc.: Natick, MA, USA, 2015.
25. Sreenivas, G.; Mahesh, P.; Mahalakshmi, D.V.; Kanchana, A.L.; Chandra, N.; Patra, P.K.; Raja, P.; Sesha Sai, M.V.R.; Sripada, S.; Rao, P.V.N.; et al. Seasonal and annual variations of CO_2 and CH_4 at Shadnagar, a semi-urban site. *Sci. Total Environ.* **2022**, *819*, 153114. [CrossRef]
26. Wei, C.; Wang, M.; Fu, Q.; Dai, C.; Huang, R.; Bao, Q. Temporal characteristics of greenhouse gases, (CO_2 and CH_4) in the megacity Shanghai, China: Association with air pollutants and meteorological conditions. *Atmos. Res.* **2020**, *235*, 104759. [CrossRef]
27. Fujita, R.; Morimoto, S.; Maksyutov, S.; Kim, H.S.; Arshinov, M.; Brailsford, G.; Aoki, S.; Nakazawa, T. Global and regional CH_4 emissions for 1995–2013 derived from atmospheric CH_4, $\delta^{13}C$–CH_4, and δD–CH_4 observations and a chemical transport model. *J. Geophys. Res. Atmos.* **2020**, *125*, e2020JD032903. [CrossRef]
28. Feng, X.; Wei, S.; Wang, S. Temperature inversions in the atmospheric boundary layer and lower troposphere over the Sichuan Basin, China: Climatology and impacts on air pollution. *Sci. Total Environ.* **2020**, *726*, 138579. [CrossRef]
29. Fang, S.; Du, R.; Qi, B.; Ma, Q.; Zhang, G.; Chen, B.; Li, J. Variation of carbon dioxide mole fraction at a typical urban area in the Yangtze River Delta, China. *Atmos. Res.* **2022**, *265*, 105884. [CrossRef]
30. Cao, G.M.; Xu, X.L.; Long, R.J.; Wang, Q.L.; Wang, C.T.; Du, Y.G.; Zhao, X.Q. Methane emissions by alpine plant communities in the Qinghai-Tibet Plateau. *Biol. Lett.* **2008**, *4*, 681–684. [CrossRef]
31. Frankenberg, C.; Thorpe, A.K.; Thompson, D.R.; Hulley, G.; Kort, E.A.; Vance, N.; Borchardt, J.; Krings, T.; Gerilowski, K.; Sweeney, C.; et al. Airborne methane remote measurements reveal heavy-tail flux distribution in Four Corners region. *Proc. Natl. Acad. Sci. USA* **2016**, *113*, 9734–9739. [CrossRef]
32. Zhang, Z.; Guo, Y.; Wang, D.; Li, G.; Peng, D. A Noisy-OR gate based fuzzy fault tree approach for micro-leakage evaluation of bolt-gasket-flange connection, (BGFC). *J. Loss Prev. Process Ind.* **2021**, *71*, 104521. [CrossRef]
33. Yiweil, Z.; Ming, X.; Xingchun, L.; Guangquan, L.; Shuangxing, L.; Xuewen, S. Application of Vehicle-mounted Methane Detection Method in the Oil and Gas Industry. *Environ. Prot. Oil Gas. Fields* **2021**, *31*, 1–6, 10.